HHS Public Access

Author manuscript

Mater Res Express. Author manuscript; available in PMC 2021 February 17.

Published in final edited form as:

Mater Res Express. 2019 December ; 6(12): . doi:10.1088/2053-1591/ab597a.

Non-invasive acoustic fabrication methods to enhance collagen hydrogel bioactivity

Emma G Norris[1], **Joseph Majeski**[2], **Sarah E Wayson**[2], **Holly Coleman**[2], **Regine Choe**[2], **Diane Dalecki**[2], **Denise C Hocking**[1,2]

[1]Department of Pharmacology and Physiology, University of Rochester, Rochester, New York, 14642, United States of America

[2]Department of Biomedical Engineering, University of Rochester, Rochester, New York, 14642, United States of America

Abstract

Much attention has focused recently on utilizing components of the extracellular matrix (ECM) as natural building blocks for a variety of tissue engineering applications and regenerative medicine therapies. Consequently, new fabrication methods are being sought to enable molecular control over the structural characteristics of ECM molecules in order to improve their biological function. Exposing soluble collagen to acoustic forces associated with ultrasound propagation produces localized variations in collagen microfiber organization that in turn, promote cell behaviors essential for tissue regeneration, including cell migration and matrix remodeling. In the present study, mechanisms by which ultrasound interacts with polymerizing collagen to produce functional changes in collagen microstructure were investigated. The rate of collagen polymerization was manipulated by adjusting the pH of collagen solutions and the temperature at which gels were polymerized. Results demonstrate that the phase transition of type I collagen from fluid to gel triggered a simultaneous increase in acoustic absorption. This phase transition of collagen involves the lateral growth of early-stage collagen microfibrils and importantly, corresponded to a defined period of time during which exposure to ultrasound introduced both structural and functional changes to the resultant collagen hydrogels. Together, these experiments isolated a critical window in the collagen fiber assembly process during which mechanical forces associated with ultrasound propagation are effective in producing structural changes that underlie the ability of acoustically-modified collagen hydrogels to stimulate cell migration. These results demonstrate that changes in material properties associated with collagen polymerization are a fundamental component of the mechanism by which acoustic forces modify collagen biomaterials to enhance biological function.

denise_hocking@urmc.rochester.edu.

Declarations of interest

none

Research data

Data will be made available upon request.

Keywords

ultrasound; collagen; acoustics; biofabrication; tissue engineering

1. Introduction

Tissue engineering is a diverse and multidisciplinary field that combines methodologies of cell biology, chemistry, and engineering towards the goal of creating novel biomaterials that effectively capture the structural and functional properties of native tissues [1]. These fabrication strategies often employ biocompatible scaffolding materials with modifications designed to stimulate regenerative cell behaviors [1, 2]. Engineered scaffolds maybe constructed from synthetic polymers and/or native glycoprotein components of the extracellular matrix (ECM) [2]. Type I collagen is the most abundant protein in the ECM and has proven to be a valuable scaffold material due to its high availability, low antigenicity, and ability to self-assemble into three-dimensional (3D) hydrogels *in vitro* [2, 3]. However, collagen hydrogels lack many of the critical tissue-specific and local structural variations that characterize native ECMs and drive cell behaviors [4, 5]. Therefore, techniques that have the capacity to manipulate collagen structure with temporal and spatial specificity have become essential to the development of improved biomaterials having greater functionality and complexity [6].

In vitro, collagen polymerization is a hierarchical process involving successive steps of initiation, lateral association and linear extension [7]. The kinetics of collagen fibril assembly are described by a cooperative nucleation-growth mechanism that begins with monomeric collagen molecules of ~300 nm in length [8]. During collagen fibril assembly, collagen molecules self-associate longitudinally through electrostatic and hydrophobic interactions to form short nanofibrils that serve as nucleation centers for polymerization [9]. The length of this nucleation phase is both temperature and pH sensitive, and can be extended with lower temperatures and the use of acidic reaction conditions [10]. Nucleation is followed by an exponential growth phase during which higher-order collagen fibrils form through the lateral association and linear extension of microfibrils [11]. Self-assembled collagen fibers exhibit many of the structural features of native ECM collagen, including fiber diameter and periodicity [10]. However, hydrogels assembled from purified collagen differ from native ECM fibrils in several critical ways, including a lack of local, tissue-specific structural variations and the co-deposition of other ECM components [4, 5].

Recently, a number of ultrasound-based technologies have emerged to advance biomaterial fabrication [12–15]. Ultrasound fields can interact with biomaterials through thermal and/or mechanical mechanisms [16, 17]. Absorption of ultrasound results in the conversion of ultrasonic energy to heat. Ultrasound-induced temperature rises are dependent on several factors, including material properties, ultrasound exposure parameters, and beam and scanning configurations. In addition, ultrasound can exert localized compression, tensile, and shear forces via mechanical mechanisms, such as radiation force, acoustic streaming, and cavitation [16, 17]. Ultrasound fields are highly controllable with regard to frequency, pressure amplitude, pulsing parameters, and exposure duration, thus allowing the design of

optimized exposure scenarios for a variety of different systems and biomaterials. For collagen-based biomaterials, the use of acoustic forces to control the structure and organization of collagen fibers is of particular interest, as non-invasive and site-specific control of collagen fiber microstructure during fabrication has the potential to direct downstream cellular responses essential to tissue remodeling and integration [15, 18].

Previous efforts at developing ultrasound-based methodologies to control collagen structure and function have yielded an exposure paradigm in which polymerization of collagen hydrogels in the presence of ultrasound produces changes in collagen fiber organization and microstructure via thermal [15] and non-thermal [18] acoustic mechanisms. Acoustically-modified collagen hydrogels demonstrated enhanced bioactivity, including increased cell migration and collagen fiber remodeling versus sham-exposed gels [18]. A key aspect of ultrasound-assisted hydrogel fabrication is that cells are not exposed directly to ultrasound but rather, seeded onto acoustically-modified hydrogels post-fabrication. Thus, understanding the mechanisms by which ultrasound interacts with collagen during hydrogel production is essential for optimizing fabrication parameters to enhance the functionality of collagen-based materials for regenerative medicine applications. In the current study, we isolate the critical stage in the collagen polymerization process during which the mechanical forces associated with ultrasound propagation are effective in producing structural changes that underlie the ability of acoustically-modified collagen hydrogels to support increased levels of cell migration.

2. Materials and methods

2.1 Generation and calibration of acoustic fields

Ultrasound fields were generated as described previously [18]. Briefly, an unfocused piezoceramic transducer with a diameter of either 0.6 cm (7.8 MHz fundamental frequency) or 1.0 cm (8.8 MHz fundamental frequency) was mounted at the bottom of a plastic exposure tank and used to generate acoustic fields within a chamber filled with degassed, deionized water. Transducers were driven using a continuous sinusoidal signal at their respective fundamental frequencies. Acoustic fields were calibrated in the free field before and after each experiment using a needle (Onda, HNC-0400) or capsule (Onda, HGL-0085) hydrophone. The peak positive and negative amplitudes, as well as spatial peak, pulse average intensity (I_{sppa}) as measured with the capsule hydrophone, are reported for each exposure condition (table 1). An exposure position was selected for each transducer based on measurements of the acoustic pressure as a function of spatial location such that the half-maximal transaxial beam width was 3 mm (4.9 cmfromthe7.8-MHz and 10.5 cm from the 8.8-MHz transducer). The waveforms measured at both locations demonstrated characteristic features of nonlinear acoustic propagation, including asymmetry in the amplitude of the peak positive and peak negative pressures, and the presence of harmonic frequency components above the fundamental frequency [19, 20].

2.2. Collagen gel preparation

Native type I collagen gels were prepared as described previously [15]. Briefly, degassed solutions of Dulbecco’s modified Eagle’s medium (DMEM, Invitrogen) or PBS were

combined with type I rat tail collagen (Corning) such that the final concentrations were 0.8, 1.0 or 2.0 mg ml^{-1} collagen [21] and 15 mMHEPES in 1X DMEM or PBS. In some experiments, collagen polymerization was inhibited by adding acetic acid to a final concentration of 0.02 N (final gel pH = 6.1). For optical turbidity measurements, phenol red-free DMEM (Invitrogen) was used in place of DMEM to minimize baseline absorbance. To reduce the probability of cavitation, media was degassed in a vacuum chamber prior to mixing. Collagen was maintained in its unpolymerized state prior to acoustic exposures by pre-chilling all reagents to 4 °C and maintaining the solutions on ice. Collagen polymerization was initiated by transferring the cold solutions to a pre-warmed exposure chamber.

2.3. Fabrication of acoustically modified collagen hydrogels

Acoustically-modified collagen gels were fabricated within modified elastomer-bottomed tissue culture plates as described previously [15]. Briefly, tissue culture plates were positioned at the surface of the exposure chamber water bath using a three-axis positioner (Series B4000, Unislide; Velmex) such that the well was centered at the acoustic calibration location. An aliquot of neutralized collagen (0.8 mg ml^{-1}) solution was then added and allowed to polymerize for 15 min in the presence of continuous wave ultrasound (8.8-MHz fundamental frequency with an acoustic intensity of 7.9 W cm^{-2} unless otherwise indicated). A frequency of ~8 MHz was chosen in order to provide a narrow beam width for good spatial resolution of the affected area. An intensity that provided maximum effect of ultrasound on collagen microstructure was chosen based on previous work investigating the dependence of the effect on acoustic intensity [18]. The presence of a fluid-air interface generated an ultrasound standing wave field within the sample during exposure. However, previous experiments found no differences in the final structure of collagen fibrils at nodes and antinodes within the ultrasound-exposed volume [15]. Sham-exposed samples were polymerized under identical conditions in the absence of ultrasound.

To alter the rate of collagen polymerization [10], the water temperature in the exposure chamber was adjusted to 13, 18, 25, or 37 °C. To analyze the temporal relationship between the stage of collagen fiber assembly and ultrasound-induced bioeffects, aliquots of neutralized collagen solution were added to exposure wells and samples were exposed for 5 min at an initial location. At the 5 and 10 min time points, tissue culture plates were translated transaxially through the acoustic field to a new location such that each gel was exposed to ultrasound at 3 separate locations (with a separation distance of 5 mm) for 5 min each. The cumulative exposure time for all samples was 15 min. Sham-exposed samples were similarly translated through the exposure chamber in the absence of ultrasound. Following exposures, collagen gels were incubated for an additional 1 h at 37 °C, 8% CO_2. Cell culture media (AimV, Gibco and SF Media, Corning in a 1:1 ratio) was then added and gels were incubated overnight to allow for media equilibration. The final thickness of polymerized gels was 5 mm.

2.4. Phase contrast and multiphoton microscopy

Fibronectin-null mouse embryonic fibroblasts (FN-null MEFs) were cultured in a 1:1 mixture of AimV (Gibco) and SF medium (Corning) as described previously [15]. These

cells do not produce fibronectin endogenously and are cultured in defined media that lacks fibronectin and other adhesive proteins. Under these conditions, FN-null MEFS utilize the acoustically-modified substrate for adhesion and migration. FN-null MEFs (4.7×10^4 cells cm^{-2}) were seeded on polymerized gels and cultured at 37 °C, 8% CO_2 for 24 h. Phase contrast images were captured using a BX-60 upright microscope (Olympus) equipped with a digital camera (QImaging). Panoramic images were obtained by collecting overlapping images from the region of interest and reconstructed using Photoshop software (Adobe).

In other experiments, a cellular ultrasound- or sham-exposed collagen gels were fixed with 2% paraformaldehyde in PBS. Collagen fibers were visualized with second harmonic generation (SHG) microscopy, using a Fluoview FVMPE-RS microscope equipped with a 25X (NA 1.05) objective (Olympus). Samples were illuminated with an 800 nm light generated by a Mai Tai HP Deep See Ti:Sa laser. Emitted light was detected with a photomultiplier tube through a bandpass filter of 370–410 (collagen SHG). Images were collected at representative locations within the area of interest through a depth of 100 μm in 5-μm z-steps, beginning at the collagen gel surface. Maximum intensity axial projections were reconstructed using FIJI software (NIH). Each experimental condition included at least 3 gels fabricated on independent days; 3–5 representative images were collected from within the ultrasound-exposed region of each gel, or from the corresponding center of sham-exposed gels.

2.5. Collagen temperature measurements

The temperature of polymerizing collagen was monitored during ultrasound exposure as described previously [15]. Briefly, type-T wire thermocouples were placed within a single well of a modified tissue culture plate such that the thermocouple junction was located within the center of the well and positioned 2.5 mm above the elastomer membrane bottom. The temperature in the exposure water tank was set to 13, 18, 25, or 37 °Cas indicated, and maintained at constant temperature throughout the duration of each recording. Aliquots of soluble collagen were added to wells and exposed to ultrasound (7.8- or 8.8-MHz fundamental frequency, over an intensity range from 1.7 to 10 W cm^{-2}). Temperature was recorded every 15 s for at least 15 min using a digital thermometer (BAT-12, Physitemp).

Initial ultrasound-induced heating rates were determined using an embedded thermocouple [22]. Aliquots of soluble collagen (0.8 or 1.0 mg ml^{-1} in neutralized DMEM or acidified PBS) were added to wells and allowed to equilibrate for at least 1 h at room temperature. This time was sufficient to allow collagen polymerization to proceed within neutralized collagen samples, but not within acetic acid-treated samples. Tissue culture plates were then placed within the acoustic exposure tank such that the thermocouple was located at the acoustic calibration location. Samples were exposed to continuous wave ultrasound for at least 3 min. Temperature was recorded every 5 s using a digital thermometer (BAT-12, Physitemp), or at a 1-kHz sampling rate using a PowerLab 26T data acquisition unit controlled by LabChart software. Heating rates were calculated for the initial 15 s of each temperature curve by linear regression.

2.6. Collagen turbidity measurements

Collagen polymerization was monitored during acoustic exposures using a custom-built turbidity measurement system (figure 1 (a)). Parallel slots were cut into the walls of a single well of an elastomer-bottomed tissue culture plate and replaced with glass windows. The optical source was a 405-nm laser diode (Sanyo DL5 146–101 S, 40 mW, Moriguchi, Osaka, Japan) driven by a constant power laser driver module (Thorlabs LD1100, Newton, NJ). The laser output was coupled via an optical fiber (Thorlabs, M75L02, 200-μm diameter) into a collimating lens (Thorlabs F220SMA-B, Newton, NJ), directing the laser beam into the well. The optical signal transmitted through the well was coupled via an optical fiber bundle (Dolan-Jenner Industries B824, 3.1-mm diameter, Boxborough, MA) to a silicon photodetector (Newport 818-SL, Irvine, CA). The optical signal was monitored with a handheld optical power meter (Newport 842-PE, Irvine, CA), and recorded using LabView software (National Instruments, Austin, TX) with a 10-Hz sampling rate. Initial measurements of transmitted optical power in an empty well demonstrated a stable power output of 400 μW ± 2% over 1 h of continuous recording. A type-T wire thermocouple was placed at the center of the exposure well, 2.5 mm above the bottom membrane, and temperature measurements were recorded using a digital thermometer (BAT-12, PhysiTemp).

To monitor collagen turbidity during ultrasound exposure, the custom spectroscopic exposure plate was then placed at the water surface within the ultrasound exposure system (figure 1 (b)). The exposure plate was placed in position at the surface of the water bath such that the thermocouple junction was located at the acoustic calibration location, and equilibrated to water bath temperature for at least 20 min prior to the start of the experiment. Cold aliquots of soluble collagen (0.8 mg ml^{-1} in DMEM) or vehicle control (DMEM) were added to the exposure plate such that the fluid level within the well was above the laser path. Samples were exposed to continuous wave ultrasound at a center frequency of 8.8 MHz (7.9 W cm^{-2}), or exposed to sham conditions, for 20 min. Optical and temperature measurements were collected simultaneously during ultrasound exposures, followed by an additional 10 min data collection period after ultrasound was turned off. Relative turbidity was calculated as the optical absorbance (A) across a 3.7-cm beam path, using equation (1):

$$A = -\log\frac{I}{I_o} \tag{1}$$

where I is the optical power transmitted across the collagen sample, and I_o is the optical power transmitted across an empty well [23]. At a collagen concentration of 0.8 mg ml^{-1}, turbidity is directly proportional to collagen fibril mass [10]. Controls included wells filled with DMEM alone to assess stability of the optical signal in the absence of collagen. For polymerizing collagen samples, the end of lag phase was defined as the time point at which relative turbidity exceeded 3 standard deviations above the mean value recorded in DMEM-only samples.

2.7. High-frequency acoustic attenuation measurements

The effect of collagen polymerization on acoustic attenuation was measured in a room temperature water tank using a fixed-path, pulse-echo approach [24]. A single-element, PVDF, focused transducer (PI50-2, Olympus) was driven by a pulser/receiver (5073PR; Olympus) and recorded by a digital oscilloscope (Waverunner 62Xi-A, LeCroy). This transducer has a focal distance of 21 mm, with a center frequency of 38 MHz (half-maximal bandwidth 13–47 MHz). Additional characteristics of this transducer in an equivalent setup have been described [25]. The transducer angle was adjusted to maximize the acoustic signal generated by reflections from a steel reflector at the focus, which was positioned 7 cm away from the transducer face during pulse-echo interrogation of samples.

Sample chambers were fabricated from polystyrene tubes (4-cm length, 1.7-cm diameter; Corning), with one end enclosed by a Saran membrane. Chambers were filled with sample (2.0 mg ml^{-1} collagen in DMEM or 0.02 N acetic acid, or vehicle alone). Sample chambers were then sealed with a second Saran membrane and inserted into the acoustic propagation path such that the focus was located 1 cm below the upper membrane. Pulse-echo data (A-lines) were collected from the same location every 30 s for up to 20 min following sample addition. The signal received from the steel reflector was isolated from each A-line beginning 6 min after sample addition (i.e., a time point prior to the initiation of collagen fibril assembly), and the maximum amplitude of this echo was recorded at each subsequent time point.

2.8. Statistical analyses

All statistical analyses were performed using Prism software (Version 8, GraphPad) and are presented as mean ± SEM for $n \geqslant 3$ samples per condition on at least 3 independent days. Mean values for polymerized versus unpolymerized samples were compared using a two-tailed t-test. Where multiple comparisons were performed, t-tests were followed by Holm-Sidak's post-hoc test.

3. Results

3.1. Heating profiles of polymerizing collagen solutions during ultrasound exposure

Ultrasound exposure (7.8 or 8.8 MHz, 3.2–10 W cm^{-2}) during collagen polymerization produces multiple characteristic changes in the collagen fiber structure of the resulting hydrogels [18]. Characteristic features of acoustically-modified collagen hydrogels include radial fiber alignment, increased collagen fiber density, and networks of interconnected pores [18]. These structural changes, in turn, support a coordinated cellular response that includes reduced adhesion, increased directional cell migration, and enhanced cell-mediated remodeling of the underlying collagen substrate [18]. A representative image illustrating the cellular migration response (figure 2(a)) in the area surrounding the center of the acoustic beam (figure 2(a); black asterisk) is shown. Cells migrate into linear aggregates (white arrows), leaving behind cell-free regions (white asterisks). In contrast, cells cultured on collagen hydrogels fabricated in the absence of ultrasound remain homogeneously distributed across the gel surface [18].

To investigate the interaction of ultrasound with collagen during fiber self-assembly, the temperature within polymerizing collagen samples was measured during exposure to ultrasound and compared to sham exposures. Collagen polymerization was initiated by transferring an aliquot of neutralized collagen solution into a temperature-controlled exposure chamber. In the absence of ultrasound, heat transfer from the water bath caused the temperature at the center of the sample to rise from 6 to 23 °C (figure 2(b), sham). Exposing neutralized collagen solutions to continuous wave ultrasound (7.8 MHz, 10 W cm^{-2}) accelerated initial heating and increased the maximum temperature achieved to 29 °C. Importantly, heating in ultrasound-exposed samples proceeded in two distinct stages. During the first stage, the temperature equilibrated to 26 °C after 5 min of ultrasound exposure. This was followed by a second stage of heating beginning ~7 min into the exposure, that led to the final peak temperature of 29 °C (figure 2(c), pH = 7.4).

To determine whether collagen fiber assembly was necessary for the second stage of ultrasound-induced heating, collagen polymerization was inhibited by reducing the pH of the collagen sample. Temperatures within both polymerizing (pH = 7.4) and non-polymerizing (pH = 6.1) collagen aliquots increased at the same rate for the first 7 min of ultrasound exposure (figure 2(c)). However, non-polymerizing samples did not undergo the second stage of ultrasound-induced heating, instead maintaining a stable temperature of 26 °C for the remainder of the acoustic exposure (figure 2(c), pH = 6.1). These results indicate that the second stage of ultrasound-induced heating depends upon the ability of collagen to transition from soluble to gel phase.

We next asked whether the ability of ultrasound to introduce morphological changes to collagen microstructure coincides with the onset of the second stage of ultrasound-induced heating. Aliquots of neutralized, soluble collagen were transferred to exposure chambers to initiate collagen polymerization. Collagen polymerization was allowed to proceed for the full 15 min, but samples were exposed to ultrasound (8.8 MHz, 7.9 W cm^{-2}) for 5 min only, during 1 of 3 non-overlapping time periods spanning the polymerization process: 0–5, 5–10, or 10–15 min. For these studies, the exposure bath temperature was set to 25 °C, so that the second stage of ultrasound-induced heating would occur during the 5–10 min exposure window (figure 2(b)). Collagen fiber morphology was analyzed using SHG microscopy. As shown in figure 3, a 5-min exposure to ultrasound was sufficient to introduce characteristic changes to collagen microstructure [18], including spatial variations in collagen fiber density and increased pore size (figure 3; panel #2). Moreover, these morphological changes were introduced only during the time period marked by the second stage of ultrasound-induced heating (figure 3; 5–10 min). The microstructure of collagen hydrogels exposed to ultrasound during either the 0–5 min or 10–15 min periods of collagen fibril assembly was similar to sham-exposed collagen hydrogels (figure 3).

3.2. Pro-migratory effects of ultrasound are induced during a critical window of collagen polymerization

To examine further the relationship between collagen fibril polymerization and ultrasound-induced heating, the rate of collagen polymerization was altered by adjusting the reaction temperature. Aliquots of neutralized collagen solutions were polymerized in the presence of

8.8-MHz ultrasound at an intensity of 7.9 W cm^{-2}, with the water temperature of the exposure chamber set to 13, 18, 25, or 37 °C. As shown in figure 4(a), lower reaction temperatures and hence, reduced rates of collagen polymerization [10], led to corresponding delays in the onset of the second stage of ultrasound-induced heating. Neutralized collagen solutions exposed to ultrasound in a 13 °C water bath reached an equilibrium temperature of ~14 °C after 5 min of exposure and thus, as expected [10], did not polymerize during the 20-min exposure period; of note, these non-polymerizing samples did not exhibit the second stage of ultrasound-induced heating (figure 4(a) 13 °C). The sensitivity of the second stage of ultrasound-induced heating to the reaction rate of collagen polymerization provides additional evidence that the second stage of ultrasound-induced heating is dependent upon collagen fiber assembly.

We next asked if ultrasound exposure at different stages of collagen fiber assembly would similarly influence the cell migration response to acoustically-modified gels. To do so, collagen gels were exposed to 8.8-MHz ultrasound (7.9 W cm^{-2}) for 5 min at each of 3 spatially distinct locations; a schematic of the approach is shown in figure 4(b). Using the heating profile data shown in figure 4(a), the water bath temperature (and hence, collagen polymerization rate) was adjusted so that the second stage of ultrasound-induced heating occurred during 1 of the 3 exposure locations; that is, for bath temperatures of 37 °C, 25 °C, or 18 °C, the second stage of heating would occur during the exposure interval of 0–5 min, 5–10 min, or 10–15 min, respectively. The distribution of FN-null MEFs cultured on the surface of polymerized gels was assessed 24 h post-seeding for enhanced cell migration, indicated by the presence of large cell-free areas on the surface as cells aggregate within collagen fibril bundles [18]. As shown in figure 5, increased cell migration was observed only at locations that coincided temporally with the second stage of ultrasound-induced heating. In contrast, cells remained homogenously distributed at locations exposed to ultrasound either after (figure 5, 37 °C: positions #2 and #3; 25 °C: position #3), or before (figure 5, 25 °C: position #1; 18 °C: positions #1 and #2) the time frame in which the second stage of heating occurred. Furthermore, no migratory response was observed on collagen gels either exposed to ultrasound at low temperature and then allowed to polymerize post exposure (figure 5, 13 °C), or polymerized in the absence of ultrasound (figure 5, 25 °C sham). Together, these data demonstrate that a 5 min exposure to ultrasound is sufficient to produce collagen hydrogels that support global cell migration, but only when the exposure coincides with the stage of collagen fiber assembly marked by the second stage of ultrasound-induced heating.

3.3. Increase in acoustic absorption coincides with collagen microfibril growth

Collagen polymerization is a progressive assembly process involving successive steps of initiation, lateral association, and linear extension [7]. The kinetics of collagen polymerization *in vitro* have been studied extensively by a number of groups using optical turbidity measurements [7, 10, 23]. Thus, a custom-built, optical turbidity sensor was incorporated into the tissue culture plate and ultrasound exposure system in order to determine when the second stage of ultrasound-induced heating occurs with respect to collagen fiber assembly.

The turbidity and temperature of polymerizing collagen samples or vehicle controls were monitored simultaneously in the absence or presence of 8.8-MHz ultrasound (7.9 W cm^{-2}). For both ultrasound- and sham-exposed collagen samples, turbidity increased with time until a plateau was reached (figure 6(a)). In contrast, turbidity was negligible and remained constant in wells containing DMEM alone (figure 6(b)). The onset of the second stage of ultrasound-induced heating occurred in tandem with the increase in turbidity that signals the transition of collagen from the nucleation phase to the growth phase of fiber assembly (figure 6 (a), solid grayline). This phase transition corresponds biochemically to the onset of lateral association of thin fibrils (2–3 nm diameter) into larger fiber bundles upwards of 100 nm in diameter [7, 26]. In contrast, control samples containing media alone showed no change in relative turbidity over the duration of the experiment (figure 6(b)). Additionally, ultrasound exposure accelerated the rate of collagen polymerization, as evidenced by the left-shift in optical turbidity recordings (figure 6(a), blue lines). The earlier onset of collagen fibril assembly in ultrasound-exposed samples likely arises from the more rapid increase in temperature with ultrasound exposure (figure 6(a), red lines) [10]. Together, these results indicate that the critical window during which ultrasound induces functional changes in collagen microstructure corresponds to the stage in which lateral association of early-stage fibrils form interconnected networks of collagen fiber bundles.

3.4. Collagen fiber assembly increases the acoustic absorption coefficient to enhance ultrasound-induced heating

Absorption of acoustic energy by the polymerizing collagen sample may influence heating rates in two distinct ways. First, conversion of acoustic energy to heat results in a direct temperature increase within the propagation medium that is dependent upon both the acoustic absorption coefficient (α), and the acoustic intensity [22]. Alternatively, radiation forces associated with sound propagation within a fluid medium can result in fluid streaming, which in turn could accelerate heat exchange with the surrounding environment [27]. Therefore, we next sought to dissect the mechanisms by which collagen polymerization influences ultrasound-mediated heating through further consideration of these component contributions.

A change in acoustic absorption during collagen polymerization could arise either from ultrasound-mediated effects on collagen monomer structure (e.g., denaturation), or from ultrasound-independent changes in the acoustic absorption properties of the material (e.g., the assembly of large molecular mass collagen fibers). To determine if ultrasound alters the acoustic absorption properties of collagen monomers directly, collagen samples were polymerized in either the absence (sham) or presence of 7.8-MHz ultrasound (10 W cm^{-2}) and then allowed to re-equilibrate to room temperature. Next, ultrasound-mediated heating profiles were obtained on fully polymerized gels (figure 7(a)) and initial heating rates determined (figure 7(b)). No differences in initial ultrasound-induced heating rates were observed between ultrasound- and sham-fabricated gels (figure 7(b)), indicating that ultrasound does not directly alter the acoustic absorption properties of collagen monomers.

We next investigated the dependence of acoustic absorption on collagen fiber assembly. The temperature within collagen solutions was monitored during exposure to 8.8-MHz

ultrasound at intensities of 1.7, 3.6, or 7.9 W cm^{-2} for collagen formulations that either permitted (figure 8(a), neutralized DMEM) or prevented (figure 8(b), 0.02 N acetic acid in PBS) collagen polymerization. The initial ultrasound-induced heating rates of polymerized collagen gels were significantly increased compared to non-polymerized samples except at the lowest acoustic intensity tested (figure 8(c)). Specifically, the initial heating rate during exposure to 8.8-MHz ultrasound at 7.9 W cm^{-2} was 0.15 ± 0.03 °C s^{-1} compared to 0.04 ± 0.01 °C s^{-1} for non-polymerizing collagen solutions. At intensities less than 7.9 W cm^{-2}, the magnitude of ultrasound-induced heating was not sufficient to provide reliable measurements of acoustic absorption for non-polymerizing collagen solutions. The nonlinear relationship between initial heating rate and acoustic intensity observed in polymerized collagen gels (figure 8(c), solidbars) is consistent with previous descriptions of nonlinear acoustic absorption [19].

Thus far, results support the premise that the second stage of ultrasound-induced heating observed in polymerizing collagen samples is due to an increase in the material acoustic absorption coefficient. To provide additional evidence, acoustic attenuation of collagen samples was measured using a pulse-echo approach [24]. This method uses small-amplitude pulses of ultrasound with short pulse duration (28 ns) to minimize the generation of fluid streaming within the sample. The amplitude of acoustic echoes received through an 8-cm path containing neutralized collagen solutions declined steadily over the course of collagen polymerization (figure 9(a), solid red). In contrast, no change was observed in the echo amplitude received through non-polymerizing collagen solutions (figure 9(a), solid black), or vehicle control samples (figure 9(a), dashed lines). The echo amplitude received through collagen samples post-polymerization was 60% of the initial value, compared to greater than 90% for non-polymerizing samples (figure 9(b)). Taken together, these data indicate that collagen fiber assembly results in enhanced acoustic absorption, resulting in a second stage of ultrasound-induced heating that coincides with the assembly of large-molecular weight collagen fibers. Moreover, this shift in acoustic absorption can be utilized under various polymerization conditions to identify the critical exposure window during which effects of ultrasound on collagen hydrogel bioactivity may be introduced.

4. Discussion

Exposing collagen solutions to ultrasound during collagen fiber assembly produces changes in collagen fiber microstructure that, in turn, support enhanced cell migration and matrix remodeling [18]. In the present study, a critical window of collagen fiber assembly was identified during which pro-migratory effects of ultrasound can be produced. This temporal window corresponded to a key transition step in collagen fiber assembly, during which thin collagen nanofibrils undergo lateral association into microfibril bundles that ultimately form the basis of mature, interconnected fiber networks. The absence of either microstructural changes or biological responses to collagen hydrogels exposed to ultrasound just prior to this phase transition suggests that these structural and functional effects arise from an ultrasound-mediated change in the hierarchical organization of collagen fibers, rather than a direct effect of ultrasound on the conformation of individual collagen monomers.

A series of mechanistic studies revealed that the critical acoustic exposure window coincides with an increase in the acoustic absorption coefficient, which occurs during the fluid-to-gel transition of collagen. The increase in acoustic absorption by collagen fibers as they co-assemble into larger fibrils resulted in the second stage of ultrasound-induced heating. This result is consistent with previous demonstrations that inter-molecular interactions are a significant contributor to the overall acoustic absorption of a material [28, 29]. It is important to note that while ultrasound exposure at frequencies and intensities used in the current study produced significant heating within polymerizing collagen samples, the ability of acoustically-modified collagen gels to support cell migration was largely independent of polymerization temperature (figure 5). Rather, the increase in acoustic absorption of nascent collagen fibrils produces a characteristic increase in temperature that in turn, clearly identifies the collagen assembly phase during which acoustic forces can be used to enhance the bioactivity of collagen hydrogels.

Biomedical ultrasound is a versatile technique for manipulating the structure of collagen-based scaffolds to produce biomaterials that stimulate cellular functions necessary for tissue regeneration, including cell migration and ECM remodeling [15]. A potential application of this technique is in the production of a cellular dressings to facilitate repair of hard-to-heal wounds, including those associated with chronic diabetes, vascular disease, or severe tissue injury [2, 30]. Space-filling materials are of particular interest for wounds with deep or irregular tissue margins, where conventional sheet or gauze dressings are not sufficient to cover the entire wound area [31]. Furthermore, gaps in wound dressings are susceptible to fluid accumulation and infection [31]. Therefore, therapeutic biomaterials that can be applied to irregular wounds in soluble form and allowed to polymerize *in situ* are of significant utility [32]. The non-invasive, non-destructive ultrasound fabrication technology presented herein provides temporal and spatial specificity such that relatively short acoustic exposures could be employed in a clinical setting. As one example, application of soluble collagen to a wound could be followed immediately with direct, point-of-care ultrasound exposure to induce functional enhancement of the collagen dressing.

5. Conclusions

Ultrasound-based technologies hold significant potential for the functional manipulation of collagen fiber architecture in a variety of experimental and clinical settings. The present study identified a critical temporal window that corresponds to the active stage of collagen microfibril assembly, during which effects of ultrasound on collagen fiber structure and bioactivity are produced. Moreover, the increase in acoustic absorption that occurs during collagen fiber formation, triggers a characteristic rise in temperature that maybe used under different fabrication conditions to identify the critical acoustic exposure window for producing functional enhancement of collagen hydrogels. As such, the versatility of acoustically-modified collagen hydrogels may extend to point-of-care applications that employ ultrasound exposure in *situ*, to increase the bioactivity of collagen-based, space-filling hydrogels for treatment of complex or irregular wounds.

Acknowledgments

This work was supported by National Institutes of Health (NIH) Grants R01 EB018210 and R01 AG058746. EG N received support from the John R Murlin Memorial Fund through the Department of Pharmacology and Physiology at the University of Rochester.

Abbreviations

ECM
extracellular matrix

3D
three dimensional

pulse average intensity, I_{sppa}
spatial peak

SHG
second harmonic generation

References

[1]. Langer R and Vacanti JP 1993 Tissue engineering Science 260 920–6 [PubMed: 8493529]

[2]. Abou Neel EA, Bozec L, Knowles JC, Syed O, Mudera V, Day R and Keun Hyun J2013 Collagen—emerging collagen based therapies hit the patient Adv. Drug Delivery Rev 65 429–56

[3]. Kadler KE, Baldock C, Bella JandBoot-Handford RP 2007 Collagens at a glance J. Cell Sci 120 1955–8 [PubMed: 17550969]

[4]. Cen L, Liu W, Cui L, Zhang W and Cao Y2008 Collagen tissue engineering: development of novel biomaterials and applications Pediatr Res 63 492–6 [PubMed: 18427293]

[5]. Schleifenbaum S. et al. 2016; A cellularization-induced changes in tensile properties are organ specific—an *in-vitro* mechanical and structural analysis of porcine soft tissues. PLoS One. 11:e0151223. [PubMed: 26960134]

[6]. Antoine EE, Vlachos PP and Rylander MN2014 Review of collagen I hydrogels for bioengineered tissue microenvironments: characterization of mechanics, structure, and transport Tissue Eng Part B: Reviews 20 683–96

[7]. Gelman RA, Williams BR and Piez KA1979 Collagen fibril formation: evidence for a multistep process J. Biol. Chem 254 180–6 [PubMed: 758319]

[8]. Na GC, Butz LJ and Carroll RJ1986 Mechanism of *in vitro* collagen fibril assembly. Kinetic and morphological studies J. Biol. Chem 261 12290–9 [PubMed: 3745187]

[9]. Rosenblatt J, Devereux B and Wallace DG 1994 Injectable collagen as a pH-sensitive hydrogel Biomaterials 15 985–95 [PubMed: 7841296]

[10]. Williams BR, Gelman RA, Poppke DC and Piez K 1978 Collagen fibril formation. Optimal *in vitro* conditions and preliminary kinetic results J. Biol. Chem 253 6578–85 [PubMed: 28330]

[11]. Gale M, Pollanen MS, Markiewicz P and Goh MC 1995 Sequential assembly of collagen revealed by atomic force microscopy Biophys. J 68 2124–8 [PubMed: 7612856]

[12]. Comeau ES, Hocking DC and Dalecki D 2017 Ultrasound patterning technologies for studying vascular morphogenesis in 3D J. Cell Sci 130 232–42 [PubMed: 27789577]

[13]. Dalecki D and Hocking DC 2015 Ultrasound technologies for biomaterials fabrication and imaging Ann. Biomed. Eng 43 747–61 [PubMed: 25326439]

[14]. Garvin KA, Hocking DC and Dalecki D 2010 Controlling the spatial organization of cells and extracellular matrix proteins in engineered tissues using ultrasound standing wave fields Ultrasound Med. Biol 36 1919–32 [PubMed: 20870341]

[15]. Garvin KA, VanderBurgh J, Hocking DC and Dalecki D2013 Controlling collagen fiber microstructure in three-dimensional hydrogels using ultrasound J. Acoust. Soc. Am 1341491–502

[16]. Dalecki D 2004 Mechanical bioeffects of ultrasound Annu. Rev. Biomed. Eng 6 229–48 [PubMed: 15255769]

[17]. National Council on Radiation Protections and Measurements, Scientific Committee 66 on Biological Effects of Ultrasound 2002 Exposure Criteria for Medical Diagnostic Ultrasound: II. Criteria Based on All Known Mechanisms (Bethesda, MD: National Council on Radiation Protection and Measurements)

[18]. Norris EG, Dalecki D and Hocking DC 2019Acoustic modification of collagen hydrogels facilitates cellular remodeling Materials Today Bio. 3 100018

[19]. Dalecki D, Carstensen EL, Parker KJ and Bacon DR1991 Absorption of finite amplitude focused ultrasound J. Acoust. Soc. Am 89 2435–47 [PubMed: 1861004]

[20]. Muir TG and Carstensen EL1980 Prediction of nonlinear acoustic effects at biomedical frequencies and intensities Ultrasound Med. Biol 6 345–57 [PubMed: 7222267]

[21]. Kreger ST, Bell BJ, Bailey J, Stites E, Kuske J, Waisner B and Voytik-Harbin SL2010 Polymerization and matrix physical properties as important design considerations for soluble collagen formulations Biopolymers 93 690–707 [PubMed: 20235198]

[22]. Fry WJ and Fry RB 1954 Determination of absolute sound levels and acoustic absorption coefficients by thermocouple probes—theory J. Acoust. Soc. Am 26 294–310

[23]. Zhu J and Kaufman L2014 Collagen I self-assembly: revealing the developing structures that generate turbidity Biophys. J 1061822–31

[24]. Bamber JC 1998 Ultrasonic properties of tissues ed Duck FA, Bdaker AC and Starritt HC Ultrasound in Medicine (Philadelphia (PA): Institute of Physics Publishing) pp 57–88

[25]. Mercado KP, Helguera M, Hocking DC and Dalecki D 2014 Estimating cell concentration in three-dimensional engineered tissues using high frequency quantitative ultrasound Ann. Biomed. Eng 42 1292–304 [PubMed: 24627179]

[26]. Bard JBL and Chapman JA 1973 Diameters of collagen fibrils grown *in vitro* Nature New Biology 246 83–4 [PubMed: 4519110]

[27]. Marshall JS and Wu J2015 Acoustic streaming, fluid mixing, and particle transport by a Gaussian ultrasound beam in a cylindrical container Phys. Fluids 27103601–103601

[28]. Kremkau FW, Carstensen EL and Aldridge WG 1973 Macromolecular interaction in the absorption of ultrasound in fixed erythrocytes J. Acoust. Soc. Am 53 1448–51 [PubMed: 4732608]

[29]. Pauly HandSchwan HP 1971 Mechanism of absorption of ultrasound in liver tissue J. Acoust. Soc. Am 50 692–9 [PubMed: 5096505]

[30]. Falanga V 2005 Wound healing and its impairment in the diabetic foot Lancet 366 1736–43 [PubMed: 16291068]

[31]. Campitiello F, Della Corte A, Guerniero R, Pellino G and Canonico S2015 Efficacy of a new flowable wound matrix in tunneled and cavity ulcers: a preliminary report Wounds 27152–7

[32]. Sood A, Granick MS and Tomaselli NL2014 Wound dressings and comparative effectiveness data Adv Wound Care 3 511–29

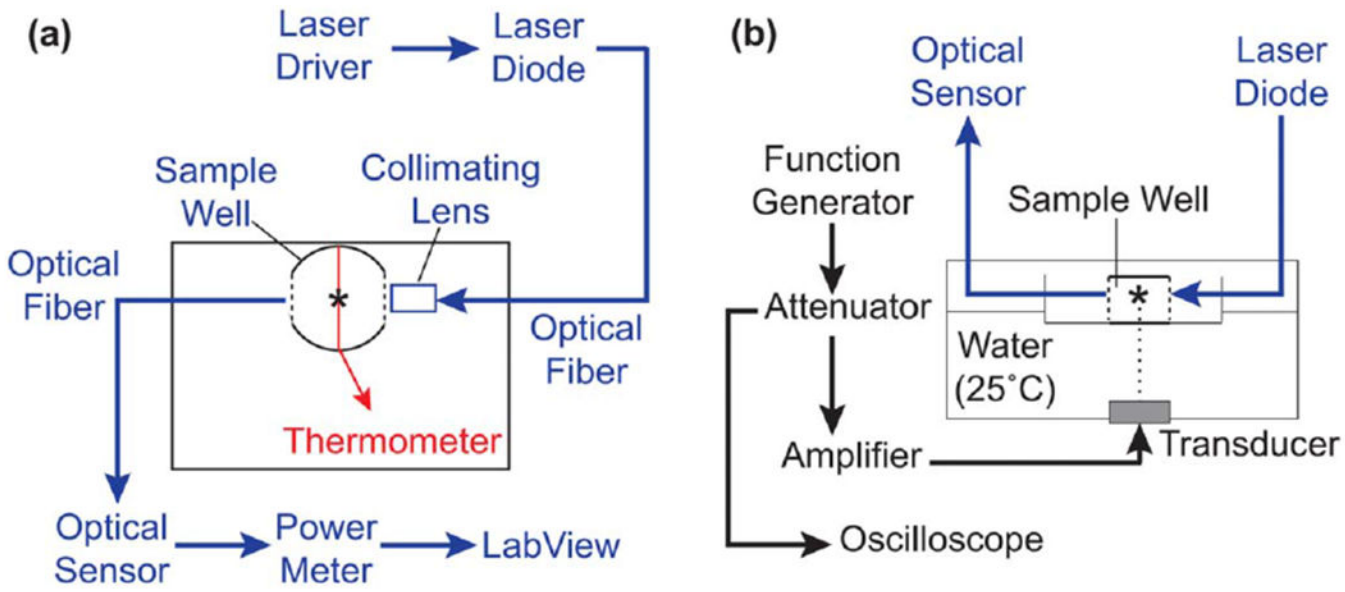

Figure 1.

Schematic of optical monitoring system for ultrasound-exposed collagen (a) Top-down view of ultrasound exposure system illustrating components of the optical and temperature monitoring systems. Parallel sides of the plastic well were cut out and replaced with glass windows (dashed lines). Light from a 405-nm laser diode was directed into the collagen sample via a collimating lens and received on the opposite side by an optical sensor. Optical power measurements were acquired by LabView software. A type-T wire thermocouple (red line) was placed below the optical beam path and the temperature of the sample monitored by a digital thermometer. The spectroscopy plate was placed in an ultrasound exposure chamber such that the thermocouple junction and light paths coincided with the 3-mm ultrasound beam (asterisk), (b) Ultrasound fields (8.8 MHz, 7.9 W cm^{-2}) were generated using an unfocused piezoceramic transducer mounted at the bottom of a temperature-controlled water bath. The plate was allowed to equilibrate to water bath temperature prior to sample addition. Black, ultrasound exposure system; blue, optical monitoring system; red, temperature monitoring system.

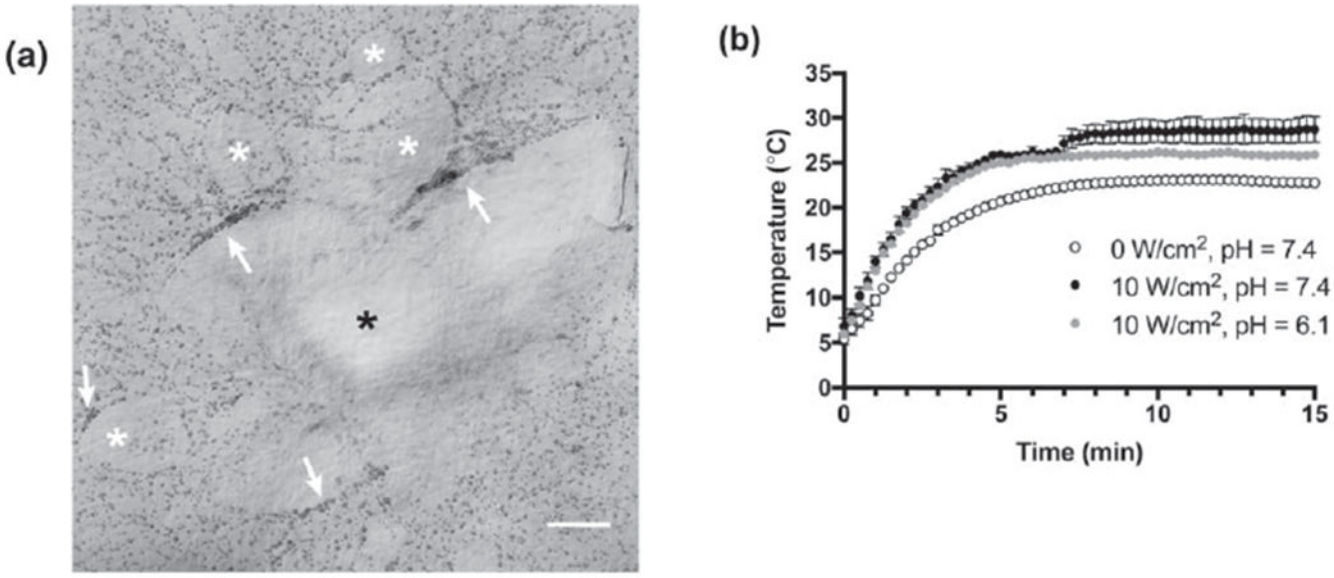

Figure 2.

Effect of collagen polymerization on ultrasound-induced heating (a) Representative image illustrating the cellular response to acoustically-modified collagen hydrogels. FN-null MEFs (4.7×10^4 cells cm^{-2}) were seeded on the surface of collagen gels polymerized in the presence of 8.8-MHz ultrasound for 15 min (7.9 W cm^{-2}). Following 24 h of culture, cells on the surface of acoustically-modified collagen gels migrated into large linear aggregates (white arrows), leaving behind cell-free areas (white asterisks). Black asterisk indicates the center of the acoustic beam. Scale bar = 500 μm. (b) The temperature of collagen (0.8 mg ml^{-1}) was measured at the center of the acoustic beam during exposure to 7.8-MHz ultrasound at an intensity of 0 (sham, open circles) or 10 W cm^{-2} (filled circles). Collagen solutions were prepared in DMEM and the pH adjusted to either 6.1 (gray), or 7.4 (black) with 0.02 N acetic acid. All exposures were conducted in a chamber with the water temperature set to 25 °C. Temperature was recorded every 15 s for the duration of the exposure. Data are presented as mean ± SEM for n ⩾ 3 replicates per condition.

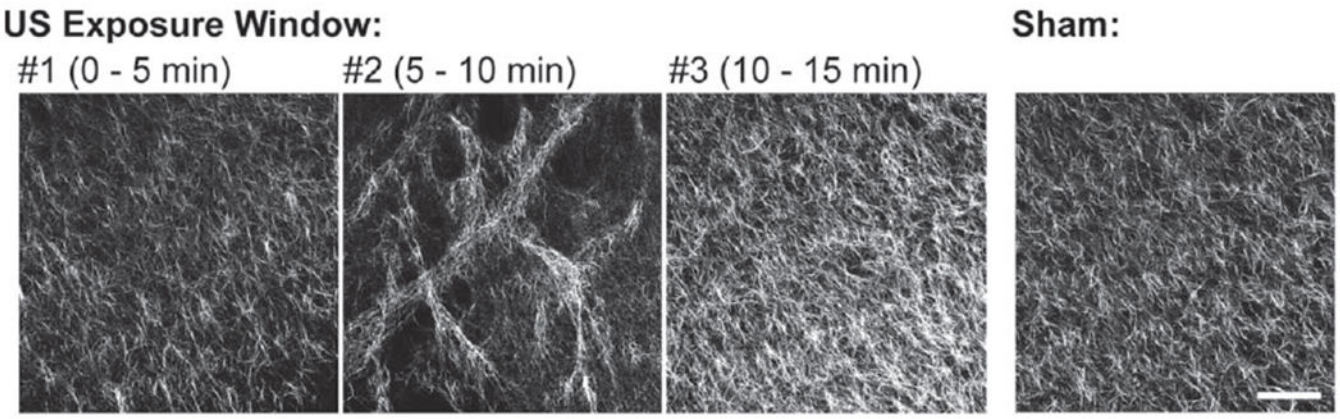

Figure 3.

Aliquots of neutralized soluble collagen (0.8 mg ml^{-1}) were transferred to exposure plates positioned in a 25 °C water bath. Collagen polymerization was initiated, and samples were exposed to ultrasound (8.8 MHz, 7.9 W cm^{-2}) for 5 min during 1 of 3 non-overlapping time periods spanning the polymerization process: 0–5, 5–10, or 10–15 min. Control collagen samples were sham-exposed. Polymerized gels were imaged using SHG microscopy. Maximum intensity projections were obtained through a depth of 100 μm and assembled using FIJI software. Images represent 1 of at least 3 experiments from gels fabricated on independent days. Scale bar = 100 μm.

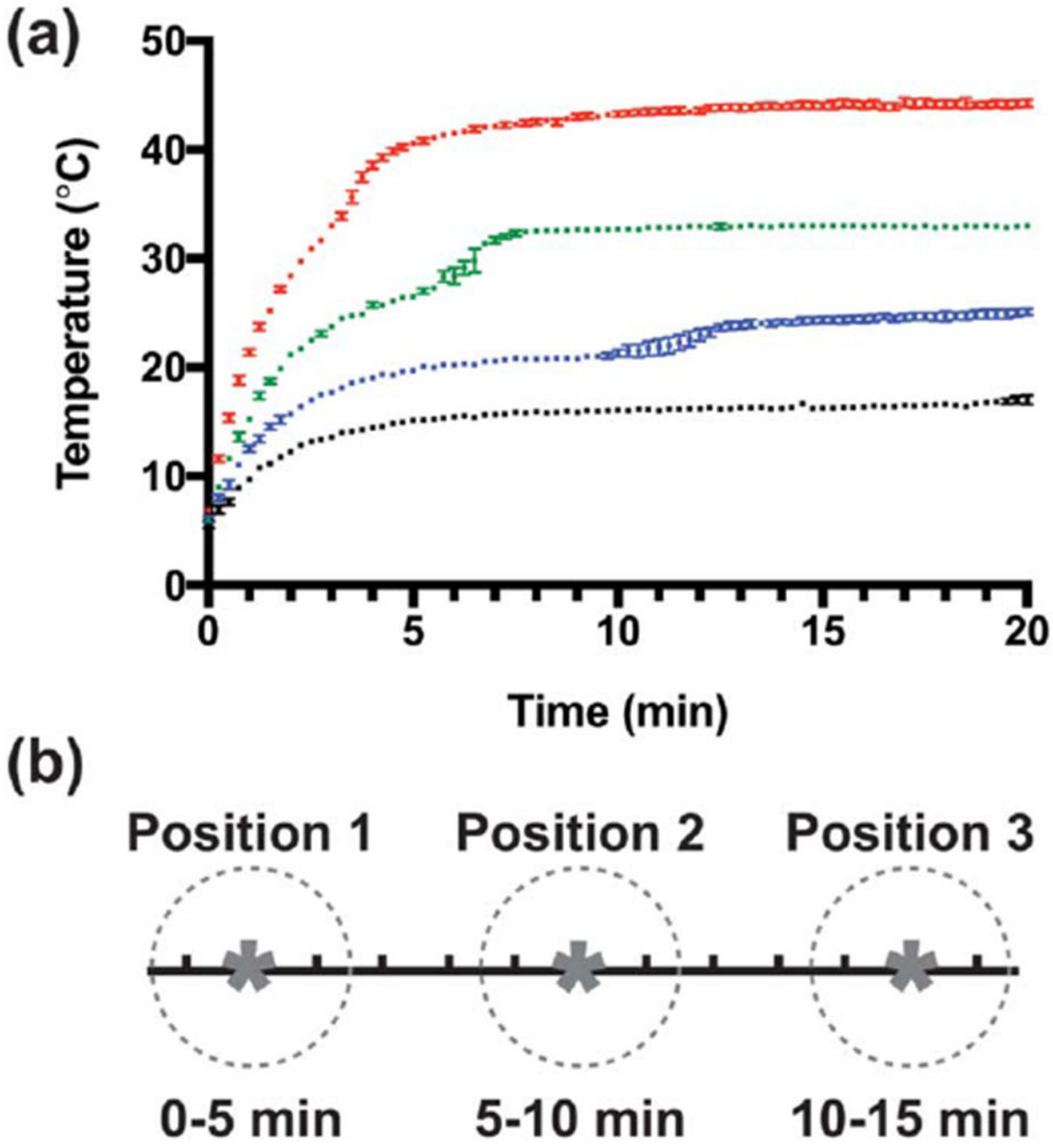

Figure 4.

Onset of second stage of ultrasound-induced heating depends on collagen polymerization rate (a) The temperature of neutralized collagen solutions (0.8 mg mL^{-1} in DMEM) was measured at the center of the acoustic beam during exposure to 8.8-MHz ultrasound (7.9 W cm^{-2}). The polymerization rate of collagen was adjusted by setting the water bath temperature to 13 (black), 18 (blue), 25 (green), or 37 °C (red). Temperature was recorded every 15 s for the duration of the exposure. Data are presented as mean ± SEM for $n \geqslant 3$ replicates per condition. (b) Schematic illustrating multipoint ultrasound exposures trategy.

Collagen solutions were exposed to 8.8-MHz ultrasound (7.9 W cm^{-2}) for 5 min at each of 3 positions (asterisks) over the course of 15 min. The half-maximal beam width of the acoustic field was 3 mm (dashed circles). The center of each exposure location (asterisks) was separated by step sizes of 5 mm to ensure no overlap between exposure locations. Scale = 1 mm/division.

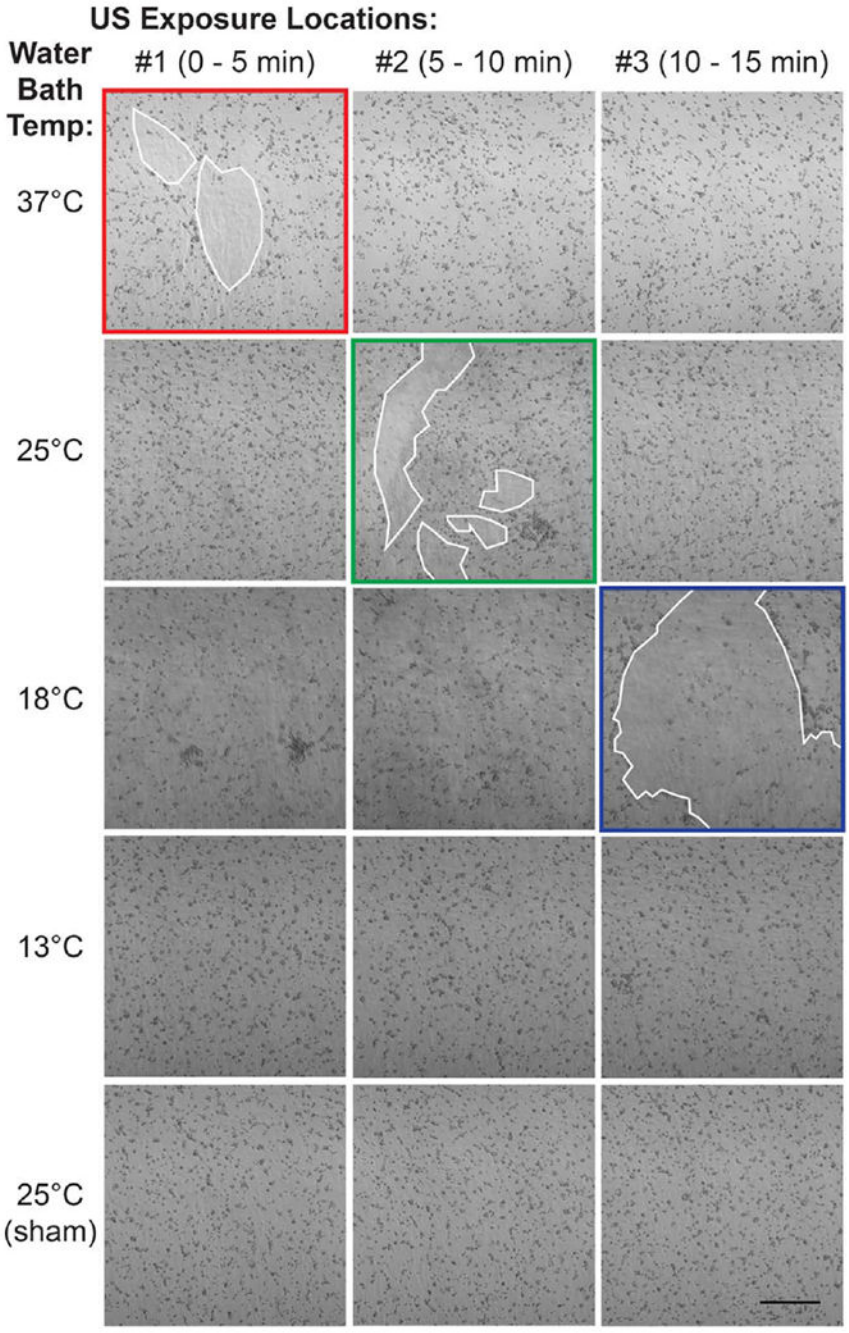

Figure 5.

Pro-migratory activity is introduced during second stage of ultrasound-induced heating. Aliquots of neutralized soluble collagen (0.8 mg ml^{-1}) were exposed to 8.8-MHz ultrasound (7.9 W cm^{-2}) or sham-exposed at 3 different, sequential locations for 5 min each, for a total exposure of l5 min. Additionally, the rate of collagen polymerization was varied by setting the water bath temperature to 37, 25, 18, or 13 °C, so that the second stage of ultrasound-induced heating coincided with the first (37 °C, red), second (25 °C, green), or third (18 °C, blue) exposure location. Collagen polymerization did not occur within the 15-min exposure

period when the temperature was set to 13 °C. All samples were allowed to polymerize fully post-exposure before FN-null MEFs (4.7×10^4 cells cm^{-2}) were seeded on gel surfaces. After 24 h, phase contrast images were captured at each of the 3 exposure locations. White outlines indicate cell-free areas on the collagen gel surface. Images represent 1 of at least 3 independent experiments. Scale bar = 500 μm.

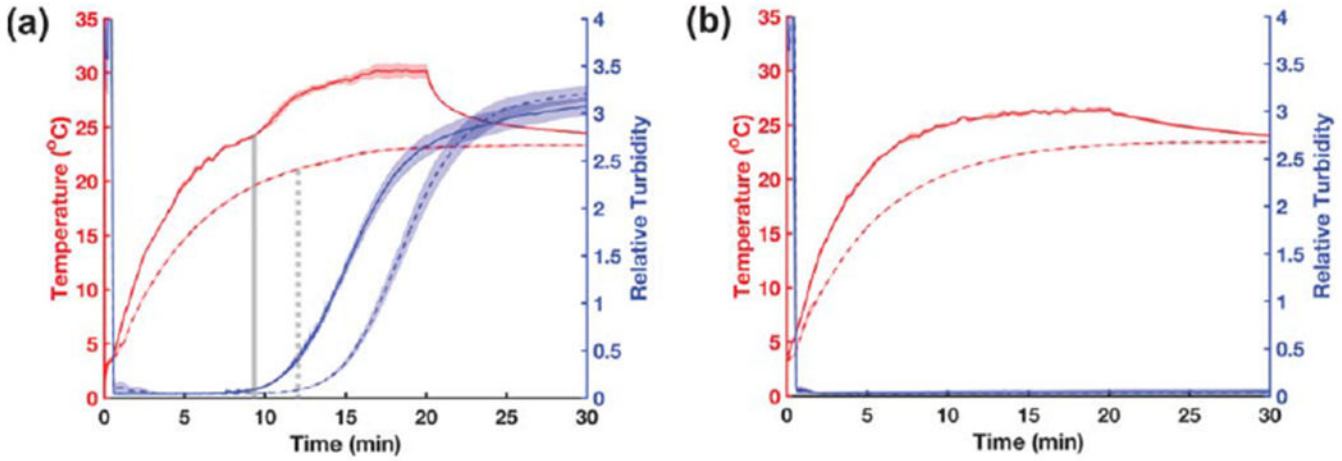

Figure 6.

Turbidity monitoring of collagen polymerization during ultrasound exposure Aliquots of neutralized collagen (a) or DMEM alone (b) were either exposed to 8.8-MHz ultrasound (solid lines, 7.9 W cm^{-2}) or sham-exposed (dashed lines, 0 W cm^{-2}) for 20 min in a 25 °C water bath; data were collected for an additional 10 min after the sound was turned off. The optical power (405 nm) transmitted across a 3.7-cm path length was recorded at a 10-Hz sampling rate. Data are presented as optical turbidity (blue) relative to transmission through an empty well. Temperature (red) at the center of each sample was simultaneously recorded every 15 s using a type-T wire thermocouple. In panel (a), vertical gray lines indicate the end of the optical lag phase for ultrasound- (solid) and sham-exposed (dashed) samples. Data are presented as mean ± SEM for n = 3 replicates per condition.

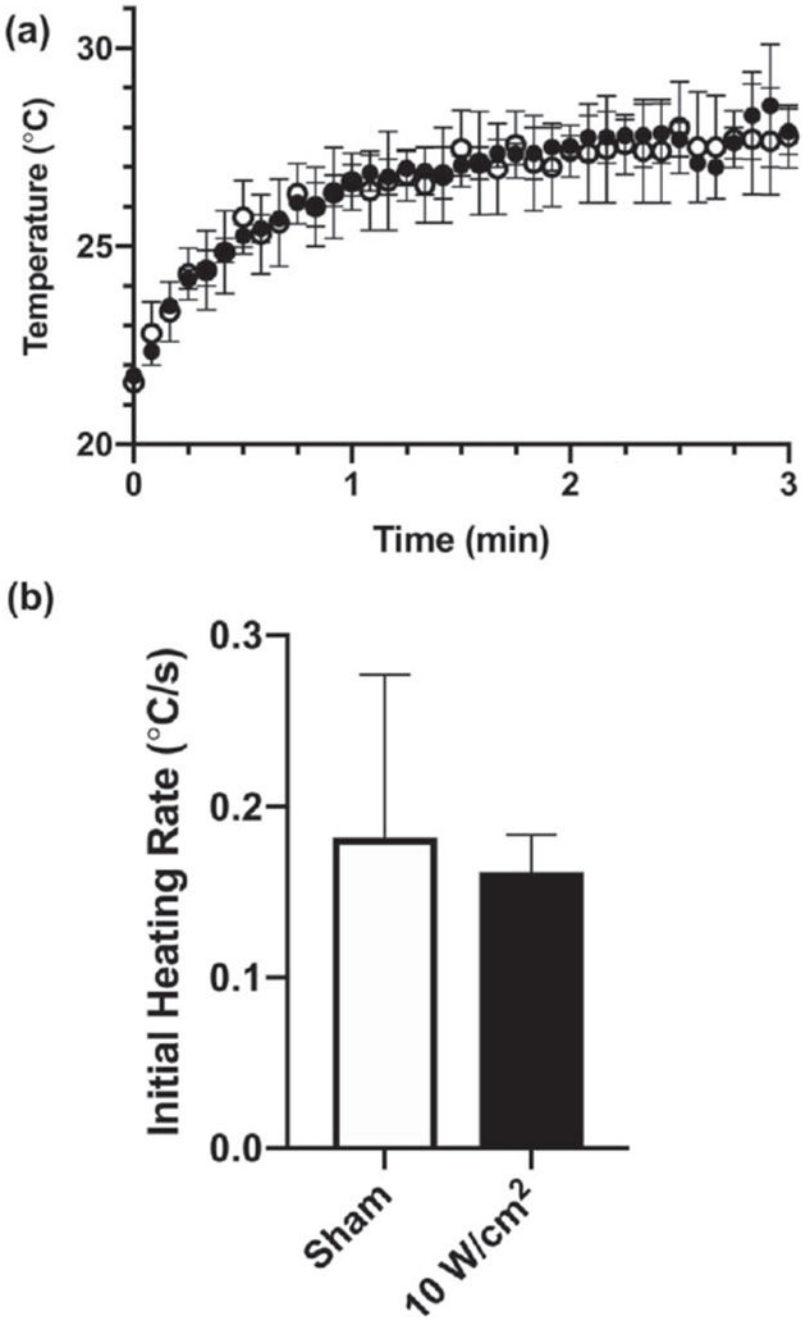

Figure 7.

Ultrasound does not alter the acoustic absorption coefficient of collagen directly. Collagen samples (0.8 mg ml^{-1}) with embedded thermocouples were first polymerized in the presence or absence of 7.8-MHz ultrasound (10 W cm^{-2}). Fully polymerized samples were then allowed to equilibrate to water bath temperature. Both non-exposed (open circles) and ultrasound-exposed (filled circles) collagen gels were subsequently heated with 7.8-MHz ultrasound (10 W cm^{-2}) and the collagen temperature within the acoustic beam was recorded every 5 s for 3 min (a). (b) The ultrasound-induced heating rate was calculated for

the initial 15 s of each recording. No differences were observed in the ultrasound-induced heating rate for collagen polymerized under sham (white), or ultrasound conditions (black).

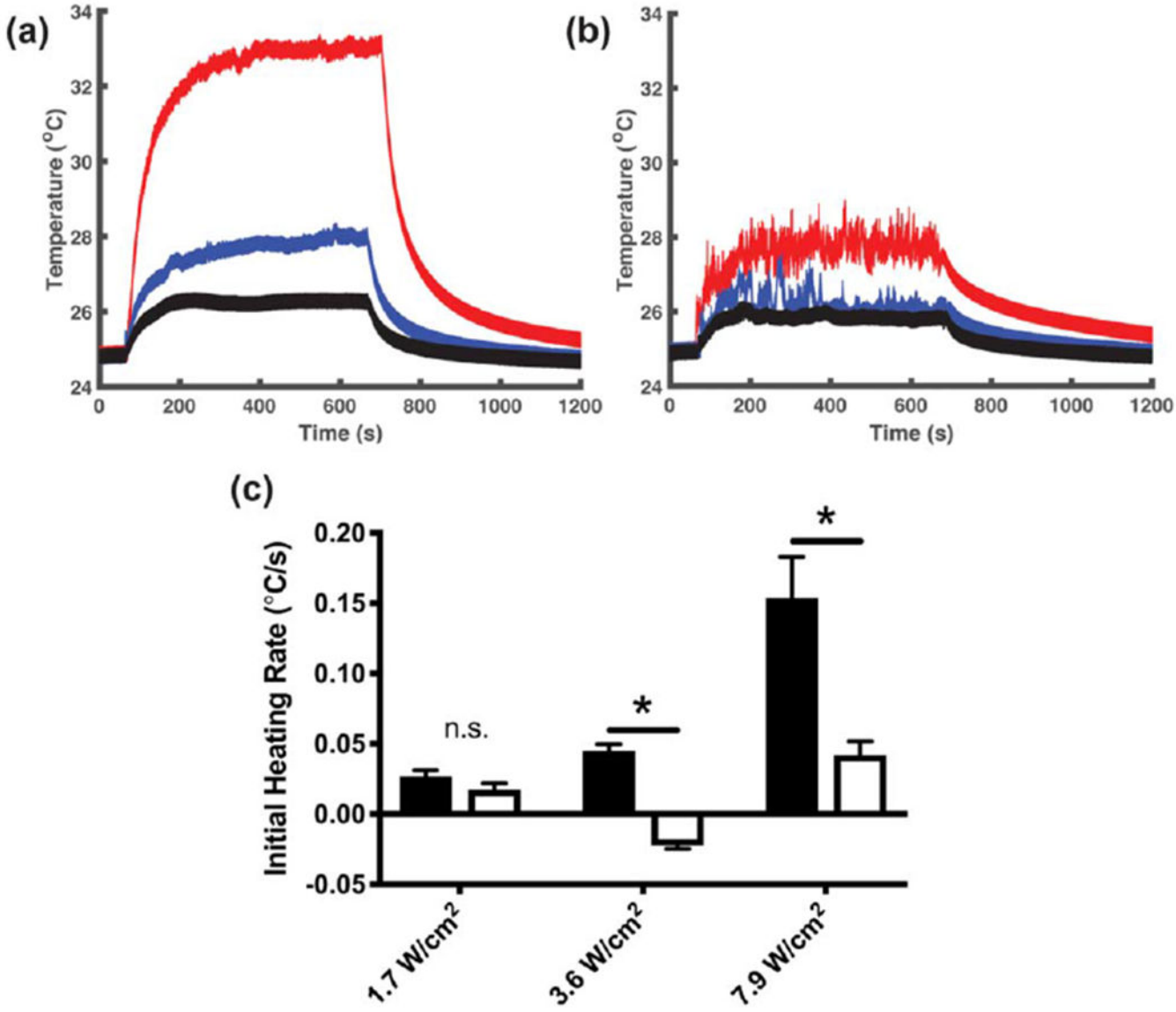

Figure 8.

Collagen fiber assembly increases the acoustic absorption coefficient. Aliquots of soluble collagen (1.0 mg ml^{-1} were transferred into the wells of modified tissue culture plates with a wire thermocouple placed at the center. Samples were allowed to equilibrate for 1 h in the absence of ultrasound. During this time, collagen polymerization either proceeded (neutralized DMEM, (a), or was prevented by maintaining acidic conditions (0.02 N acetic acid in PBS, (b). The temperature at the center of each sample was recorded during subsequent exposure to 8.8-MHz ultrasound at intensities of 1.7 (black), 3.6 (blue), and 7.9 W cm^{-2} (red). Each graph represents a set of recordings from 1 of at least 3 independent samples. (c) The initial ultrasound-induced heating rate was calculated for polymerized (black) and non-polymerized (white) samples by performing a linear regression over the first 10 s of ultrasound exposure. Data are presented as mean ± SEM for n ⩾ 4 recordings from at

least 3 independent samples per condition. Significantly different means, *P < 0.05 by t-test with Holm-Sidak's post-hoc test for multiple comparisons.

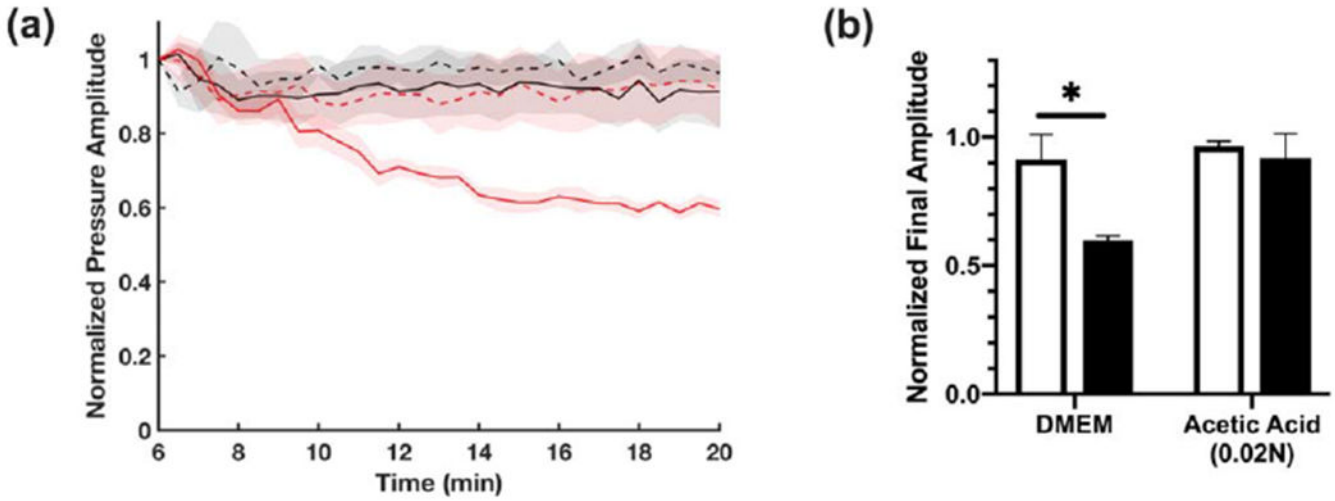

Figure 9.

Effect of collagen polymerization on acoustic attenuation (a) Aliquots of soluble collagen solution (2.0 mg ml^{-1}, solid lines) or vehicle control (dashed lines) were prepared under either neutralized (red, DMEM) or acidic (black, 0.02 N acetic acid in PBS) conditions. Cold samples were placed in a 4-cm long cylindrical sample holder with Saran membranes on either side. Acoustic attenuation measurements were obtained by a pulse-echo technique using a 28 ns ultrasound pulse (38 MHz center frequency) reflected by a steel disk placed at the bottom of the propagation path. The amplitude of the signal received from the reflector was recorded every 30 s and plotted beginning 6 min after sample addition (e.g., prior to collagen polymerization), as the normalized mean ± SEM for n ⩾ 3 replicates per condition. (b) Echo amplitude at 20 min normalized to initial amplitude (6 min) for vehicle control (white), or 2.0 mg ml^{-1} collagen (black) samples. Data are presented as mean ± SEM for n ⩾ 3 replicates per condition. Significantly different means, *$P < 0.05$ by t-test with Holm-Sidak's post-hoc test for multiple comparisons.

Table 1.

Summary of acoustic exposure conditions. Ultrasound fields were generated using an unfocused piezoceramic transducer with diameter and center frequency as indicated. Fields were calibrated using a capsule hydrophone at a position in the free field such that the half-maximum beam width was 3 mm. Data are presented as mean ± SEM for n ⩾ 6 measurements per condition on independent experimental days.

Acoustic intensity (I_{SPPA})	Peak positive pressure	Peak negative pressure
Transducer 1:0.6 cm-diameter, 7.8-MHz center frequency, exposure site = 4.9 cm from transducer		
10.0 ± 0.2 W cm^{-2}	0.65 ± 0.01 MPa	0.44 ± 0.01 MPa
Transducer 2:1-cm diameter, 8.8-MHz center frequency, exposure site = 10.5 cm from transducer		
1.7 ± 0.1 W cm^{-2}	0.28 ± 0.02 MPa	0.19 ± 0.02 MPa
3.6 ± 0.1 W cm^{-2}	0.46 ± 0.02 MPa	0.28 ± 0.02 MPa
7.9 ± 0.1 W cm^{-2}	0.74 ± 0.02 MPa	0.43 ± 0.02 MPa